Contents lists available at ScienceDirect

Materials Characterization

Microstructural, mechanical and electrochemical behaviour of a 7017 Al–Zn–Mg alloy of different tempers

Prasanta Kumar Rout *, M.M. Ghosh, K.S. Ghosh

Department of Metallurgical and Materials Engineering, National Institute of Technology (NIT), Durgapur, India

ARTICLE INFO

ABSTRACT

The aim of the investigation is to assess the microstructural features and associated physical, mechanical and electrochemical properties of a 7017 Al–Zn–Mg alloy of various tempers. A 7017 Al–Zn–Mg alloy was subjected to different ageing schedules to produce under-(T4), peak-(T6), over-(T7) and highly over-aged tempers. Optical microscopy, hardness measurement, electrical conductivity measurement, tensile testing and SEM fractographs, differential scanning calorimetry (DSC), transmission electron microscopy (TEM), and electrochemical polarization studies have been used to characterize the alloy tempers. Hardness measurement and tensile testing showed the characteristic age hardening phenomenon of aluminium alloys. Optical and TEM micrographs have revealed the variation in size of matrix strengthening η′ ($MgZn_2$) and also the size and distribution of grain boundary η ($MgZn_2$) precipitate with ageing time. DSC thermograms exhibiting exothermic and endothermic peaks indicated the characteristic solid state reaction sequence of the 7017 alloy. Potentiodynamic polarization study of the 7017 alloy of various tempers in 3.5 wt.% NaCl solution at near neutral pH showed typical active metal dissolution behaviour, but at pH 12 an active–passive–transpassive transition behaviour has been observed.

© 2015 Elsevier Inc. All rights reserved.

1. Introduction

For the last several decades, two different classes of 7xxx series aluminium alloys i.e. Al–Zn–Mg and Al–Zn–Mg–Cu have been developed for a variety of commercial applications in aerospace and automotive industries [1–3]. The aluminium alloy series response to precipitation hardening and the various ageing schedules are the key processes to achieve the required microstructures and associated properties. Usually, in Al–Zn–Mg alloys, the decomposition of super saturated solid solution (SSSS) during ageing results in simultaneous and independent formation of several second phase precipitates. In general, the precipitation sequence can be represented as [4–6]:

$$\text{Super saturated solid solution (SSSS)} \rightarrow \text{GP zones} \rightarrow \eta' \ (MgZn_2) \rightarrow \eta \ (MgZn_2).$$

(1)
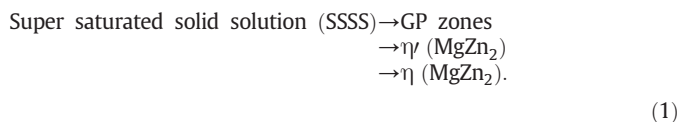
In the ternary Al–Zn–Mg alloy, the GP zones and their effects as precursors on precipitation processes have been investigated extensively by different researchers [7,8]. The η′ precipitates play major roles on the strengthening effect in Al–Zn–Mg alloy. The formation of the η′ precipitate and its variants depends on the alloy composition, artificial ageing temperature, ageing time and nucleation conditions etc. The ageing behaviour, sequence of precipitation and dissolution reactions and microstructural features of the Al–Zn–Mg alloys have been assessed by various techniques [9–14]. However, the precipitation sequence and the microstructural features comprising such a large number of metastable and stable phases are very complex and are dependent on alloy composition, solute content, Zn/Mg ratio, the presence impurities (such as Fe, Si, and Mn), processing history, solutionizing temperature, quenching severity, and artificial ageing schedule. Hence, the research for establishing the microstructural features and structure–property relationships in the 7xxx aluminium alloys is still vibrant and active till today.

7017 Al–Zn–Mg is a low copper medium strength weldable alloy and is widely used in armoured fighting vehicles, military bridges, drilling rod and in general engineering applications as well [15,16]. The mechanical properties and stress corrosion cracking (SCC) behaviour of the 7017 alloy base metal and the weld joints have been studied by different researchers [17–20]. However, there are a few literature available which have dealt with the effect of different ageing tempers and their microstructure, mechanical properties and electrochemical behaviour of the 7017 alloy [17,21].

Aluminium and its alloys (e.g. age-hardenable 2xxx, 6xxx, and 7xxx series) exposed to atmosphere form a thin and adherent oxide protective film. But, the protection against corrosion by this film is limited to environments in which it is unstable (locally or uniformly) and or even slightly soluble as well. According to Pourbaix diagram [22], passivity of aluminium is limited in the pH range of 4 to 9. However,

* Corresponding author.
E-mail addresses: prasantonnet55@yahoo.com (P.K. Rout), ksghosh2001@yahoo.co.uk (K.S. Ghosh).

the protective effect in this pH range where the oxide film seems to be stable is destroyed because of the presence of defects or discontinuities which leads to initiation of localized corrosion such as pitting corrosion, intergranular corrosion (IGC) and exfoliation corrosion in aqueous solution and in moist atmosphere containing active chloride ions [23–27].

Further, the high strength peak aged (T6) temper of the aluminium alloys is susceptible to environmental induced cracking (EIC) e.g. stress corrosion cracking (SCC), hydrogen embrittlement (HE) and corrosion fatigue (CF) in aqueous solutions containing particularly active chloride ions. Over aged tempers (e.g. T7, T73, T76) have acceptable SCC resistance but with about 10–15% lower strength than the peak aged (T6) temper [28,29], thus requiring over size component with an imposed over-weight penalty. There are many novel techniques such as retrogression and reageing (RRA) [30], interrupted ageing (T6I6) [31] and high temperature pre-precipitation (HTPP) ageing [32] schedules to alter the microstructure for retaining peak aged strength but with an improved resistance to SCC.

The chloride ion is very aggressive in nature which destroys passive layer locally in the weaker/defective portion of the protective oxide film and induce high local dissolution resulting pitting corrosion. Further, pitting in aluminium alloys is also strongly influenced by the presence of second phase precipitates and intermetallic particles which have different surface film characteristics than that of matrix. These phases and intermetallics are either anodic or cathodic in nature relative to the matrix which leads to galvanic action and dissolution/corrosion. It is reported in several literatures [33–36] that stress corrosion cracks invariably initiate from the base of the pits and or from the intergranularly corroded/denuded regions. A few literature [37–39] have also dealt with investigation of electrochemical behaviour and its effect on SCC behaviour has been studied by many researchers. However, it is very much essential to study the electrochemical behaviour of the 7xxx alloys in order to assess its corrosion resistance and also to acquaint with the electrochemical data e.g. corrosion potential (E_{corr}), corrosion current density (i_{corr}), pitting potential (E_{pit}), and repassivation potential (E_{rp}) in detail.

So, the present investigation has focused on assessing the structure–property relationship of the 7017 Al–Zn–Mg alloy of under-(T4), peak-(T6), over-(T7) and highly over-aged tempers. Hardness measurement, electrical conductivity measurement, tensile testing, SEM fractography, differential scanning calorimetry (DSC), transmission electron microscopy (TEM) and electrochemical studies have been performed to characterize the various tempers of the 7017 alloy.

2. Experimental procedures

2.1. Material

A 7017 Al–Zn–Mg aluminium alloy in plate form of 10 mm thick was obtained from Defence Metallurgical Research Laboratory (DMRL), Hyderabad, India. The chemical composition (wt.%) of the alloy is: Zn — 5.2, Mg — 2.3, Cu — 0.12, Zr — 0.13, Fe — 0.35, Si — 0.082, Mn — 0.3 and Al — balance. The alloy plate was further reduced in our laboratory to about 4 mm thickness by hot rolling, then reduced to 2 to 3 mm by cold rolling and finally the alloy sheet was stress relieved. The initial 10 mm thick alloy plate was annealed at 450 °C for 1 h and then hot rolled with an approximate 10% reduction in each pass and the plate was subjected to three passes. Again the plate was annealed at 450 °C for 0.5 h and subjected to rolling giving approximately 10% reduction in each pass for thrice. This yielded sheet of approximately 4 mm thickness. This 4 mm sheet was again annealed at 450 °C for 30 min and then cold rolled to 2 mm at room temperature with an approximate 5% reduction in each pass and subjected to four passes. The cold rolled bent 2 mm sheet was straightened followed by stress relief annealing at 200 °C for about 1 h.

2.2. Optical microstructure

For microstructural observations, specimens were ground mechanically and polished using a series of SiC emery papers up to 1500 grit. Final cloth polishing was done using 0.5 μm size particle of diamond paste. Then the specimens were degreased with ethanol, rinsed with distilled water followed by etching in Keller's reagent (95 vol.% H_2O_2, 2.5 vol.% HNO_3, 1.5 vol.% HCl and 1.0 vol.% HF). An optical microscope model LEICA DM 2500 M with an inbuilt QWIN 3 software is used to observe the microstructures of the alloy.

2.3. Solution heat treatment, ageing schedules and hardness measurement

For ageing study, specimens of dimensions of 10 mm × 10 mm × 2 mm were cut from the rolled sheet. The specimens were solution treated at 470 °C for 45 min, water quenched (WQ), followed by artificial ageing. Artificial ageing was done in an oven at 120 °C controlled to within ± 2 °C for varying time to produce various tempers i.e. under-(T4), peak-(T6) and over-aged (T7). Further, in order to produce highly over-aged temper, two-step ageing treatment was adapted, i.e. the samples were solutionized, water quenched following first ageing at 120 °C for 24 h and then ageing at 150 °C for 30 h. Hardness was measured using Vickers micro-hardness tester (Model MMT-X78, Matsuzawa Co Ltd.) using a diamond pyramid indenter at an applied load of 200 gf.

2.4. Electrical conductivity measurement

For electrical conductivity measurements, rectangular specimens were cut from the alloy sheet. Electrical conductivity test was done by a KEITHLEY Model 6221 programmable current source and Model 2182 sensitive digital voltmeter using conventional four-probe technique. A constant current was fed from one end to the other end of the rectangular sample and the voltage was measured across two contacts which were away from the current contacts in order to keep the lines of current flow uniform and parallel. The resistivity of the sample was calculated from the voltage drop, the applied current, and the geometry of the samples. In this present investigation, the authors presented the conductivity data in $\mu\Omega^{-1}\,cm^{-1}$ and as percentage of the International Annealed Copper standard (% IACS). More than three measurements were preformed for each specimen and an average value was reported.

2.5. Tensile testing and SEM fractograph

Tensile specimens with gauge dimensions of 15 mm length, 6 mm width and 2 mm thickness were prepared from the long transverse (L–T) direction of the alloy sheet. Tensile testing was carried out in a universal testing machine (INSTRON 8516) at a cross-head speed of 2 mm/min as per the ASTM E8-1983 standard. The gauge portion the specimen surfaces was ground to 100 μm minimum from the original sheet thickness in order to remove the zinc depleted surface and subsurface zones developed during heat treatments in air. The gauge portion of all the specimens was ground with a sequence of SiC paper from 220 to 1500 grit size, rinsed with distilled water, degreased with ethanol and dried prior to testing. Tests were repeated to confirm the results and the error limit is ± 5% of the reported values. The fractured surfaces of tensile tested specimens were examined in a scanning electron microscope (Model S 300N, Hitachi and JSM-5800, JEOL) operating at 15 kV. Secondary electron (SE) mode was used to examine fracture surfaces using a working distance of 27 mm.

2.6. Differential scanning calorimetry (DSC)

Differential scanning calorimetry (DSC) runs on the 7017 alloy samples of solutionized and water quenched (WQ) state was initiated from